Virtual Dermatologist: An Application of 3D Modeling to Tele-Healthcare

D. Lam* and G. N. DeSouza**
Department of Electrical and Computer Engineering
University of Missouri
349 Eng. Building West, Columbia, MO, 65211
Email: *DLam@mizzou.edu, **DeSouzaG@missouri.edu

***Abstract*—In this paper, we present preliminary results towards the development of the Virtual Dermatologist: A 3D image and tactile database for virtual examination of dermatology patients. This system, which can be installed and operated by non-dermatologists in remotes areas where access to a dermatologist is difficult, will enhance and broaden the application of tele-healthcare, and it will greatly facilitate the surveillance and consequent diagnosis of various skin diseases. Unlike other systems that monitor the progress of skin diseases using qualitative data on simple baseline (2D) photography, the proposed system will also allow for the quantitative assessment of the progress of the disease over time (e.g. thickness, size, roughness, etc). In fact, the 3D model created by the proposed system will let the dermatologist perform dermatoscopic-like examinations over specially annotated areas of the 3D model of the patient's body (i.e. higher definition areas of the 3D model). As part of its future development, the system will also allow the dermatologist to virtually touch and feel the lesion through a haptic interface. In its current form, the system can detect skin lesions smaller than 1mm, as we demonstrate in the result section.**

I. Introduction

When it comes to skin illnesses, the role of the dermatologist vis-à-vis general practitioners is undeniable. According to an Australian study by Marks et. al, [1], dermatologists are equipped to diagnose skin cancer more effectively, specifically melanoma, and the ratio of benign to malignant lesions removed is 11.7:1 for dermatologists vs. 29.9:1 for general practitioners. Unfortunately, 40% of the population in the USA has no access to dermatological care. This number is even higher in other countries and even though the higher density of dermatologist is associated with better prognosis in patients diagnosed with malignant melanoma [2], the effectiveness in the diagnostic and treatment still relies on non-dermatologists. In fact, the diagnosis of melanoma by a non-dermatologist has been associated with an increased breslow thickness and with more late stage melanomas at time of diagnosis than the diagnostic by dermatologists [3]. In the same study, median breslow thickness in melanomas diagnosed by dermatologists has been found to be significantly less (0.5mm) than by other providers.

This effectiveness in the diagnostic by dermatologists relies, amongst other things, on constant examinations [4]. That is, periodic surveillance for new or changing nevi in patients who have potential precursors of melanoma (including atypical nevi), prominent numbers of nevi, a previous melanoma, or a family history of cutaneous melanoma, is fundamental for the correct diagnostic and to improve patient outcomes [5]. In that sense, the periodic visits by a patient to a dermatologist is also very important, since the sensitivity of the visual examination by a dermatologist is 89% to 95%, with a positive predictive value of 35% to 75% for the diagnosis of melanoma [6].

Fortunately, the difficulty in access to health care and specifically to dermatologists can be minimized by the use of technology. One such example is the teledermatology system proposed in [7]. This system enables dermatology services to the patients at remote areas via distant and specialized medical sites. It uses one of the most common types of tele-healcare called store-and-forward, which is based on the concept of sharing information asynchronous and place-independent. Also, it relies on transmitting baseline photography and patient information to a distant expert who provides the consultation [8], [7].

Here, we propose a 3D modeling system that will allow for the development of the Virtual Dermatologist: A 3D image database for virtual examination of dermatology patients. This system, which can be installed and operated by non-dermatologists at remotes areas of the state and the country can provide more than just total cutaneous photography and it will greatly facilitate the surveillance and consequent diagnosis of malignant melanoma as well as other skin diseases. Unlike other systems [9], [4], that monitor the progress of such diseases using qualitative data on simple baseline (2D) photography, the proposed system will also allow for the quantitative assessment of the progress of the disease. In fact, the 3D model created by our system will let the dermatologist perform dermatoscopic-like examinations over specially annotated areas of the 3D model of the patient's body (i.e. higher definition areas of the 3D model)

II. Background

A. Teledermatology and Baseline Photography

The prospective surveillance of high risk patients with the aid of baseline photography can help identify early, thin melanomas [4] because it helps detect subtle changes, while it is non-invasive; it minimizes unnecessary surgery; it is efficient; and it is cost effective. That is, by simply being able to compare the images of the patient over a period of time, one can improve early diagnostic even for the strongest risk factor for the development of melanoma, which is the presence of a large number of benign nevi [10], [11], [12], [13]. Moreover,

978-1-61284-696-5/11/$26.00 ©2011 IEEE

total cutaneous photography can guide the physician in the examination, while it can aid in the detection of clinically subtle, early malignant melanoma. Also, the use of baseline photography along with dermatoscopy is associated with low biopsy rates and early detection of melanoma [14]. In a study by Feit et al [9], 74% (20 out of 27) of newly diagnosed melanomas could be biopsied because of changes detected using simple baseline photography. In patients with dysplastic nevus syndrome, photographic surveillance has been shown to increase early diagnosis of melanoma and is much more cost-effective than prophylactic excision of atypical nevi [12]. Not to mention that total cutaneous photography can also reduce the excision of benign lesions and alleviate patient anxiety, reducing medical costs. In a study by Banky [14], it was found that less than 1% of new or changed nevus detected by total cutaneous photography were indeed melanoma in patients younger than 50 yrs and 30% were melanomas in patients above 50 yrs.

B. 3D Modeling

Object modeling has a wide range of applications in several areas such as: robotics [15], [16], virtual reality [17], [18], medicine and health care [19], [20]. In the latter case, creating 3D models of the human body can pose a great challenge due to the lack of texture in the human skin. This problem forces the use of unconventional methods, that is, methods that are not based only on intensity correlation. Hence, many approaches involving constrained global optimizations of photometric discrepancy functions have appeared in the literature recently. Some of these works were surveyed, evaluated, and can be found in [21]. In [22], for example, the authors reported a successful reconstruction of the human body using multi-view. However, the method, which was based on the detection of boundary motion extracted from the level set, still required specialized parallel PC hardware and software for efficient use of computation resources (e.g. load balancing). Other methods, such as [23], proposed a deformable model for 3D reconstruction of the human face. In this work, while the use of a reference face did away with the intensity correlation problem by aligning and warping the reference model with the observed face, their approach could only capture geometric properties of the face. So, additional post-processing for texture mapping was required in order to achieve a realistic representation of the face. Other more traditional approaches required active sensors, like range scanners, structured-light scanners, and similar techniques [24], [25], [26]. Those methods produced high quality models through the use of a controlled light source, such as a laser. However, the trade off was usually the high computational cost and the long time required for image acquisition.

III. Design objective

In this work, we propose a new method for 3D modeling that uses multiple virtual views from a single stereo pair. Our approach, while it is multi-view based, does not require a large number of calibrated cameras positioned around the object. Instead, our method only requires a single pair of calibrated cameras and a motion detection algorithm that estimates the position of virtual cameras as the object moves with respect to such cameras. Besides the much lower cost and despite the much simpler setup, the 3D models created using this approach is highly comparable to the original Patch-based Multiview Stereo (PMVS) algorithm, while maintaining the same computational efficiency. Also, as the original PMVS, our method works well on various objects, including human faces, as we demonstrate in the results section. Another great advantage of our method is in the simplicity to obtain denser models if necessary: by only increasing the number of sampled images during that object-camera motion.

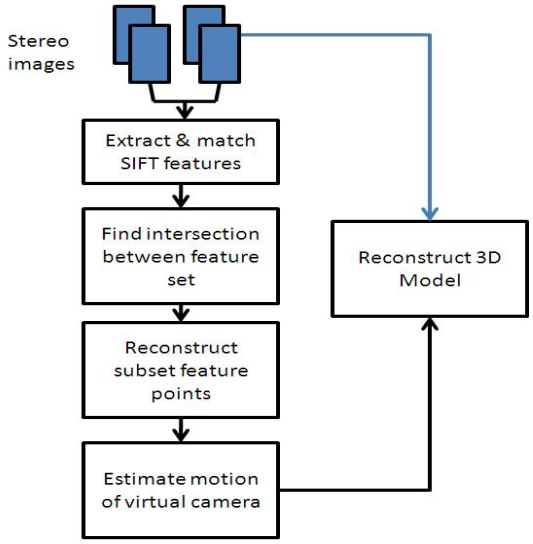

Figure 1: Proposed Framework for Virtual Multi-View 3D Modeling

IV. System Description

The proposed framework takes a hybrid approach to the reconstruction of the human body. On one hand, the motion of the virtual stereo cameras have to be computed using structure from motion (SfM) algorithms. Once the location of the virtual stereo cameras is known, PMVS is used to reconstruct the complete model of the human body with both geometry and texture information. The proposed framework for a virtual dermatologist can be decomposed into 6 steps: 1) Multiple pairs of images are captured by two calibrated cameras while the human rotates with respect to the cameras and the background is eliminated by the algorithm describe in [27]; 2) A SIFT-based feature extraction and matching algorithm ([28]) establishes the correspondences between images at two consecutive positions; 3) The intersection between the sets of corresponding points from two consecutive pairs of images is determined. That is, the algorithms finds identical feature points seen by the stereo cameras at two consecutive positions and create an intersection set; 4) The 3D coordinates

of every point in the intersection set above is calculated; 5) The transformation between cameras (i.e. object poses) are estimated using the 3D coordinates above; and 6) The previous transformations are used to create virtual poses of the camera and fed into a Patched-base Multi-view Stereo software ([29]) to reconstruct a 3D model of the human body.

A. Real vs. Virtual Cameras

As we explained earlier, the input images are captured by a single pair of 640x480 stereo cameras and a PC, which can be installed at any physician clinic office. The cameras are mounted on a tripod and are calibrated off-line using the CalTech Calibration Toolbox [30].

In the original PMVS method, the reconstruction algorithm also relies on a small number of calibrated cameras: in that case of [29], three cameras. However, differently from our system, their approach expands the number of views by employing a carefully-positioned turn table. That is, each camera acquires multi images of the object, while the turn table is carefully rotated at pre-defined angles. In our method, we achieve an accuracy as good as that of the original PMVS, but we rely only on two cameras and **no** turn table. Instead, in order to obtain an arbitrary number of multiple views of the object, we resort to the idea of *virtual cameras*.

In our proposed framework, our stereo cameras take images of the object as it moves freely about the camera. This motion of the object is interpreted by the algorithm as if it was the motion of the cameras. Better yet, as if the image sequence acquired by the cameras were taken by different cameras at slightly different poses: that is what we refer to as *virtual cameras*. In that sense, as the object moves in one direction, the algorithm computes the motion as if it was made by the cameras in the opposite direction. In fact, since the cameras are firmly mounted on the same tripod, there is mathematically no difference whether it is the camera or object that is actually moving. The problem becomes "simply" that of finding the pose of the virtual camera, as it is described in detail in Section IV-B

B. Motion Estimation of Virtual Camera

The most important component of the proposed frame work is how to estimate the motion, i.e. translation and rotation, of the virtual camera. Because the virtual cameras in the framework are stereo, only motion of the left virtual camera has to be estimated. Also, rather than estimating the motion of all cameras at once, we take an incremental approach in which we find the motion of the cameras from one position to the next position in the chain of acquired images. That is, once the first motion is estimated, a new position is taken into account until the chain is completed.

At each position, due to the use of a stereo system, 3D locations of feature points in the images can be estimated by triangulation, as described in [31]. For any two consecutive camera positions, identical features observed by both stereo cameras are collected into two sets of 3D points. Ideally,

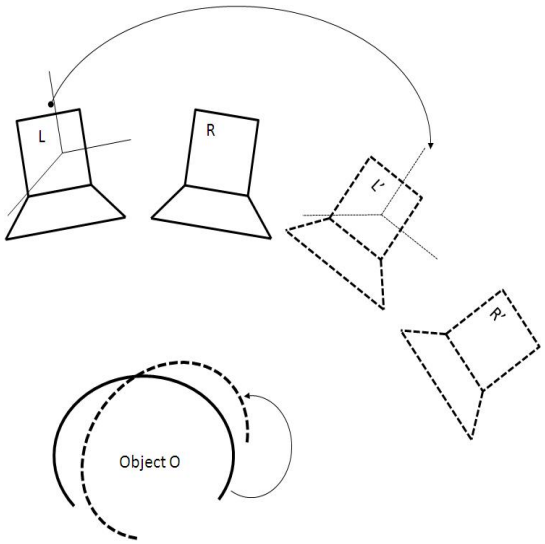

Figure 2: L,R are the real cameras, while L',R' are the estimated virtual cameras due to the motion of the object O (from solid to dotted lines).

these two sets of points contain exactly the same points of the target object, but with different coordinates due to the fact that they are being seen at different camera positions. The camera motion can be estimated by first assuming one coordinate frame fixed; then translating and rotating the second coordinate frame until the two sets of 3D points coincide. By doing so, the problem of motion estimation becomes a minimization problem, where the objective function is the sum of the distances between 3D points in one coordinate frame and its corresponding points in the transformed coordinate frame with regard to the translation and rotation of the latter coordinate frame.

C. Algorithm for Proposed Framework

The complete algorithm of the proposed framework (Figure 1) actually begins with a background subtraction using the method presented in [27]. This step is necessary because we are only interested in the human, not the background. After that, the framework finds matching points between all pairs of stereo images using the SIFT algorithm [28], [32] implemented as a Matlab toolbox [33]. Next, the framework uses two left images corresponding to two consecutive positions of the virtual cameras to establish correspondences between these positions. That is, it runs again the SIFT algorithm, but this time using the left image at position *i* and the left image at position *i+1*. By examining these three sets of points – that is, left-right at *i*, left-right at *i+1*, and left-left at *i* and *i+1* – the framework can establish the correspondence between features in space.

To compute the motion of the virtual camera, we make an assumption that the motion is rigid. That is, in this work, we assume that a simple translation and rotation can describe the movement of the feature points from position *i* and position *i+1*. From the identical features found in the previous step,

corresponding 3D sets are reconstructed. Since a motion is known to have 6 degrees of freedom, each of the 3D sets must have at least three points in order for the algorithm to be able to uniquely compute the motion. In practice, this minimization problem is solved by the iteration over a set of noisy points and therefore many more points must be obtained for better performance. The optimization used in our framework relies on the Levenberg-Marquardt approach to minimize the sum of distances between the two sets of 3D points as explained earlier.

The above procedure is repeated one pair of positions at a time until we find all the transformations between any pair of consecutive positions of the virtual cameras – i.e. two consecutive pairs of images in the acquired image chain. Since we define the first positions of the left camera to be the world reference frame, the position of any virtual left camera can be obtained by pre-multiplying the transformations of the previous virtual cameras in the chain all the way to the first position. Also, since the stereo cameras are mounted on the same tripod, their relative pose never changes in the chain and therefore, the virtual positions of the right camera can be easily derived from the positions of the left camera.

V. Experimental Results and Discussion

In this section, we present qualitative results from our virtual multi-view 3D framework when modeling the human body. Since accuracy is an important aspect of the proposed systems for diagnostic of dermatological diseases, we also compared the accuracy in 3D reconstruction by applying the algorithm to other objects whose groundtruths are known: a bunny and an angel. That is, we compare the accuracy of the model created by our method against the 3D ground truth obtained with the laser scanner presented in our previous work, [34], [26].

A. Face and Human Body Modeling

In this experiment, the person to be modeled stands in front of the cameras with his right side turned to the cameras. We start the image acquisition at 30fps while the human rotates by 180^0 in front of the cameras. Since the time to complete the 180^0 rotation and the consequent number of images acquired may vary, we sub-sampled the images by a variable factor that led to a totally of 16 images – 8 images for each camera – or one image roughly every 22.5^0.

Next, we ran the SIFT algorithm to find corresponding feature points, as explained in section IV-B. Usually, the SIFT algorithm returns about 150 matching points between left and right images, and a few dozens of other matching points between two consecutive left images. In the end, the algorithm is capable of finding between 15 and 20 points in common for each pair of consecutive positions. After running the optimization and obtaining the virtual camera poses for each of the 16 images, the same images and the calculated camera poses were input to the patch-based multi-view program. The outcome of the program for this 3D model of the human face is shown in Figure 3.

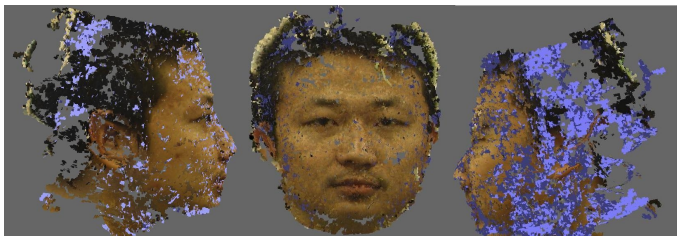

Figure 3: Reconstructed 3D face using 16 images

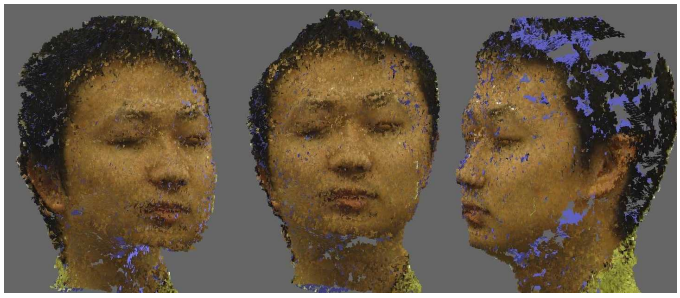

Figure 4: Reconstructed 3D face using 70 images

As we mentioned earlier, one of the major advantages of our method is in how easy it is to increase the density of a 3D model. That is, if an application requires a denser 3D model, all that one needs to do within our framework is to change the sampling factor used in the above steps. There is no need to add more calibrated cameras or to calibrate new positions of a turn table [29]. Instead, the system can make use of the images already collected in order to reduce, for example, the number of gaps in the model. As Figure 3 shows, various gaps (blue spots) are present in the 3D model, in special on the head where the low-resolution cameras used and the hair makes it harder to find feature correspondences. To reduce the number of such gaps in the model, we can increase the number of virtual poses of the cameras by simply increasing the number of sampled images after image acquisition.

Figure 4 shows such a model when 70 images were sampled. By comparing the 3D model obtained in Figure 3 and the model in Figure 4, we can see that the second model is qualitatively better than the first.

Many other similar tests were performed using the entire human body. Figure 5 presents one of such tests by showing three different views of the 3D model obtained with the proposed framework. This 3D model was created using only 28 images and greater detail of texture and geometry can be achieved with a higher number of images.

In the next section, we analyze the results in a more quantitative manner.

Figure 5: Reconstructed 3D Human Body

B. Analysis of Accuracy

In order to demonstrate the applicability of our framework in the dermatology setting, the accuracy of the 3D model needs to be very high. In that regard, we calculated the accuracy of our method by comparing it with two datasets obtained with a highly precise laser scanner ([34], [26]). Those datasets include: the angel and the bunny, which are depicted in Figure 6.

The comparison was performed by first reconstructing the 3D model of each object using the proposed framework and then using the Iterative Closest Point (ICP) [35] algorithm to match the cloud of points obtained by our method against the cloud of points from the laser scanner.

The criteria used for comparison follows the same format described in[21], however, here we concentrate only on the accuracy criterion.

Figures 6(a) and 6(b) show the real image of the two objects used, while Figure 6(c) and 6(d) show the reconstructed model using our method. The qualitative results from our algorithm is summarized in Table I. As it can be inferred from this table, our method achieves enough accuracy to detect skin lesions as small as 1mm, with a success rate of 85-90%, and lesions smaller than 1.5mm, with a rate of 93-96%.

Figure 6: Quantitative Results (a) and (b) show the images of the angel and bunny used for testing; (c) and (d) show the 3D model created using high resolution cameras.

VI. Conclusion and Future Work

In this work, we propose a novel approach to telehealthcare by building 3D models of the human body instead of more traditional baseline photography. The system, dubbed Virtual Dermatologist, uses off-the-shelf computer vision technology and state-of-the-art algorithms, allowing for the system to be installed and operated by non-dermatologists in any remote area and at a very small cost. The proposed system provides more than just total cutaneous photography and it will greatly facilitate the surveillance and consequent diagnosis of malignant melanoma as well as other skin diseases. In the future, we intend to integrate the haptic features which allow the dermatologist to virtually touch and feel the lesion.

In the future, we intend to perform a series of tests with actual wounds/molds to fully demonstrate this paper's applicability to dermatology. Also, an analysis of the model quality versus the number of input images would be very helpful to guide the user in selecting the required number of images for the desired model quality. As we already noted above, improving the method in order to reduce the holes on the model is also an important future work, which is already being conducted.

Acknowledgment

The authors would like to express their sincere gratitude to Dr. Karen Edison, chair of the Department of Dermatology, and Dr. Chi-Ren Shyu, director of the Informatics Institute, both with the University of Missouri, for their support, encouragement, and technical and professional insights.

References

[1] R. Marks, D. Jolley, C. McCormack, and A. P. Dorevitch, "Who removes pigmented skin lesions? a study of the ratio of melanoma to other benign pigmented tumors removed by different categories of physicians in australia in 1989 and 1994." *Journal of America Academy of Dermatology*, vol. 36, pp. 721–726, 1996.

[2] M. J. Eide, M. A. Weinstock, and M. A. Clark, "The association of physician-specialty density and melanoma prognosis in the united states, 1988 to 1993," *Journal of American Academy of Dermatology*, vol. 60, pp. 51–58, 2009.

[3] M. L. Pennie, S. L. Soon, J. B. Risser, E. Veledar, S. D. Culler, and S. C. Chen, "Melanoma outcomes for medicare patients: Association of stage and survival with detection by a dermatologist vs. a nondermatologist," *Archives of Dermatology*, vol. 143, 2007.

[4] R. M. Mackie, P. McHenry, and D. Hole, "Accelerated detection with prospective surveillance for cutaneous malignant melanoma in high-risk groups," *The Lancet*, vol. 341, pp. 1618–1620, 1993.

Table I: Accuracy of 3D models of the bunny, the angel

Object	Number of views	Error variance (mm)	Percentage of accuracy <1 mm	Percentage of accuracy <1.5 mm
Bunny	7	.49	85.5%	93.4%
Angel	12	1.24	89%	96%

[5] A. E. Chang, L. H. Karnell, and H. R. Menck, "The national cancer data base report on cutaneous and noncutaneous melanoma: a summary of 84,836 cases from the past decade," *Cancer*, vol. 83, no. 8, pp. 1664–1678, 1998, the American College of Surgeons Commission on Cancer and the American Cancer Society. [Online]. Available: http://dx.doi.org/10.1002/(SICI)1097-0142(19981015)83:8<1664::AID-CNCR23>3.0.CO;2-G

[6] H. K. Koh, A. Caruso, I. Gage, A. C. Geller, M. N. Prout, H. White, K. O'connor, E. M. Balash, G. Blumental, I. H. Rex, F. D. Wax, T. L. Rosenfeld, G. C. Gladstone, S. K. Shama, J. A. Koumans, G. R. Baler, and R. A. Lew, "Evaluation of melanoma/skin cancer screening in massachusetts. preliminary results," *Cancer*, vol. 65, no. 2, pp. 375–379, 1990. [Online]. Available: http://dx.doi.org/10.1002/1097-0142(19900115)65:2<375::AID-CNCR2820650233>3.0.CO;2-Z

[7] H. Pak, K. Edison, and J. Whited, *Teledermatology: A Userś Guide*. New York: Cambridge University Press, 2008.

[8] G. Demiris, S. M. Speedle, and L. L. Hicks, "Assessment of patients' acceptance of and satisfaction with teledermatology," *Journal of Medical Systems*, vol. 28, no. 6, pp. 575–579, December 2004.

[9] N. E. Feit, S. W. Dusza, and A. A. Marghoob, "Melanomas detected with the aid of total cutaneous photography," *British Journal of Dermatology*, vol. 150, pp. 706–714, 2004.

[10] J. J. Grob, J. Gouvernet, D. Aymar, A. Mostaque, M. H. R. MH, A. M. Collet, M. C. Noe, M. P. Diconstanzo, and J. J. Bonerandi, "Count of benign melanocytic nevi as a major indicator of risk for nonfamilial nodular and superficial spreading melanoma," *Cancer*, vol. 66, no. 2, pp. 387–395, Jul 1990.

[11] E. A. Holly, J. W. Kelly, S. Shpall, and S. H. Chiu, "Number of melanocytic nevi as a major risk factor for malignant melanoma," *Journal of America Academy of Dermatology*, vol. 17, pp. 459–68, 1987.

[12] J. W. Kelly, J. M. Yeatman, C. Regalia, G. Mason, and A. P. Henham, "A high incidence of melanoma found in patients with multiple dysplastic nevi by photographic surveillance." *Medical Journal of Australia*, vol. 167, no. 4, 1997.

[13] M. A. Tucker, A. Halpern, E. A. Holly, and P. Hartge, "Clinically recognized dysplastic nevi: A central risk factor for cutaneous melanoma." *Journal of America Academy of Dermatology*, vol. 277, no. 18, pp. 1439–1444, 1997.

[14] J. P. Banky, J. W. Kelly, and D. R. Endlish, "Incidence of new and changed nevi and melanomas detected using baseline images and dermoscopy in patients at high risk for melanoma," *Archives of Dermatology*, vol. 141, pp. 998–1006, 2005.

[15] G. M. Bone, A. Lambert, and M. Edwards, "Automated modeling and robotic grasping of unknown three-dimensional objects," in *International Conference on Robotics and Automation*, May 2008, pp. 292–298.

[16] M. Tomono, "3-d object map building using dense object models with sift-based recognition features," in *Intelligent Robots and Systems*, Oct 2006, pp. 1885–1890.

[17] W. S. Kim, "Computer vision assisted virtual reality calibration," *IEEE Transactions on Robotics and Automation*, vol. 15, pp. 450–464, 1999.

[18] B. Reitinger, C. Zach, and D. Schmalstieg, "Augmented reality scouting for interactive 3d reconstruction," in *Virtual Reality Conference*, 2007.

[19] A. P. Santhanam, T. R. Willoughby, I. Kaya, A. P. Shah, S. L. Meeks, J. P. Rolland, and P. A. Kupelian, "A display framework for visualizing real-time 3d lung tumor radiotherapy," *Journal of Display Technology,*, vol. 4, Dec 2008.

[20] A. C. Halpern, "The use of whole body photography in a pigmented lesion clinic," in *http://www.ncbi.nlm.nih.gov/pubmed/11134998*, 2000.

[21] S. M. Seitz, B. Curless, J. Diebel, D. Scharstein, and R. Szeliski, "A comparison and evaluation of multi-view stereo reconstruction algorithms," in *IEEE Int. Conference on Computer Vision and Pattern Recognition*, vol. 1, 2006, pp. 519–526.

[22] Y. Iwashita, R. Kurazume, R. Kurazume, S. Uchida, K. Morooka, and T. Hasegawa, "Fast 3d reconstruction of human shape and motion tracking by parallel fast level set method," in *IEEE International Conference on Robotics and Automation*, May 2008, pp. 980–986.

[23] Y. Zheng, J. Chang, Z. Zheng, and Z. Wang, "3d face reconstruction from stereo: A model based approach," in *IEEE International Conference on Image Processing*, vol. 3, 2007, pp. 65–68.

[24] M. Levoy, S. Rusinkiewicz, B. Curless, M. Ginzton, J. Ginsberg, K. Pulli, D. Koller, S. Anderson, J. Shade, L. Pereira, J. Davis, and D. Fulk, "The digital michelangelo project: 3d scanning of large statues," in *SIGGRAPH*, 2000.

[25] T. Weise, B. Leibe, and L. V. Gool, "Fast 3d scanning with automatic motion compensation," in *IEEE Int. Conference on Computer Vision and Pattern Recognition*, 2007, pp. 1–8.

[26] J. Park, G. N. **DeSouza**, and A. C. Kak, "Dual-beam structured-light scanning for 3-d object modeling," in *Proceedings of Third International Conference on 3-D Digital Imaging and Modeling*, May-Jun 2001, pp. 65–72, quebec City, Que., Canada.

[27] Y. Dong and G. N. **DeSouza** , "Adaptive learning of multi-subspace for foreground detection under illumination changes," *Journal of Computer Vision and Image Understanding*, vol. 115, no. 1, pp. 31–49, 2011.

[28] M. Brown and D. G. Lowe, "Invariant features from interest point groups." in *in the Proceedings of the British Machine Vision Conference*, 2002, cardiff, Wales.

[29] Y. Furukawa and J. Ponce, "Accurate, dense and robust multi-view stereopsis," in *Proceedings of IEEE International Conference on Computer Vision and Pattern Recognition*, 2007, pp. 1–8.

[30] J.-Y. Bouguet, "Camera calibration toolbox for matlab," http://www.vision.caltech.edu/bouguetj/.

[31] R. Hartley and A. Zisserman, *Multiple View Geometry in Computer Vision Second Edition*. Cambridge University Press, 2004.

[32] D. G. Lowe, "Distinctive image features from scale-invariant keypoints," *International Journal of Computer Vision*, vol. 60, no. 2, 2004.

[33] A. Fusiello and L. Irsara, "Quasi-euclidean uncalibrated epipolar rectification," in *International Conference on Pattern Recognition*, 2008, pp. 1–4.

[34] J. Park and G. N. **DeSouza**, *Photorealistic Modeling of Three Dimensional Objects Using Range and Reflectance Data, in Studies in Computational Intelligence, Vol. 7, Machine Learning and Robot Perception*, B. Apolloni, A. Ghosh, F. Alpaslan, L. C. Jain, and S. P. Patnaik, Eds. Springer-Verlag, 2005.

[35] S. Rusinkiewicz and M. Levoy, "Efficient variants of the icp algorithm," in *Proceedings of the Third Intern. Conf. on 3-D Digital Imaging and Modeling*, vol. 1, May 2001, pp. 145–152, quebec City, Canada.